

## Supporting Information

# Continuous Growth Phenomenon for Direct Synthesis of Monodisperse Water-soluble Iron Oxide Nanoparticles with Extraordinarily High Relaxivity

*Pohlee Cheah,<sup>a</sup> Terriona Cowan,<sup>a</sup> Rong Zhang,<sup>a</sup> Ali Fatemi-Ardekani,<sup>b</sup> Yongjian Liu,<sup>c</sup> Jie  
Zheng,<sup>c</sup> Fengxiang Han,<sup>a</sup> Yu Li,<sup>d</sup> Dongmei Cao,<sup>d</sup> Yongfeng Zhao<sup>a\*</sup>*

<sup>a</sup> Department of Chemistry, Physics and Atmospheric Science, Jackson State University,  
Jackson, MS 39217, United States

<sup>b</sup> Department of Radiology, University of Mississippi Medical Center, Jackson, MS 39217,  
United States

<sup>c</sup> Mallinckrodt Institute of Radiology, Washington University School of Medicine, St. Louis, MO  
63110, United States

<sup>d</sup> Material Characterization Center, Louisiana State University, Baton Rouge, LA 70803, United  
States

**KEYWORDS:** Continuous growth, Iron oxide nanoparticles, Water soluble, Magnetic resonance  
imaging

## **Characterization and Measurements**

### **a. Transmission electron microscope (TEM)**

The core size of nanoparticles was characterized by using transmission electron microscope (TEM) JEOL JEM-1011 (JEOL, Inc, MA). The size analysis from TEM images was performed using ImageJ software (Version 1.52a). For each sample, about 200 nanoparticles are analyzed. The statistics analysis was conducted in OriginPro 2018. High resolution TEM (HRTEM) images are obtained on JEOL JEM-2011 operating at 200 kV of accelerating voltage.

### **b. Dynamic light scattering (DLS)**

The hydrodynamic size and zeta potential of nanoparticles in water and different PBS solution were studied with dynamic light scattering (NanoZS, Malvern, Worcestershire, UK).

### **c. Fourier transform infrared (FT-IR)**

The dried nanoparticles were scanned using Perkin Elmer Fourier Transform Infrared (FT-IR) Spectrometer (Perkin Elmer, Waltham, MA) from 400-4000  $\text{cm}^{-1}$  with a resolution of 4  $\text{cm}^{-1}$  for 64 scans.

### **d. Inductively Coupled Plasma Mass Spectrometer (ICP-MS)**

The iron concentration was analyzed by using a Varian 820 Inductively Coupled Plasma Mass Spectrometer (ICP-MS) (Varian, Australia). Data collection was achieved by ICP-MS Expert software package (Version 2.2b126).

### **e. Thermogravimetric analysis (TGA)**

Thermogravimetric analysis was used to determine weight change of samples over heating process. Analysis was performed using a TA Instruments Q500 TGA and Advantage for Q Series (Version 2.5.0.256, Thermal Advantage Release 5.5.22, TA Instruments-Waters LLC).

### **f. Calculating the conversion rate of $\text{Fe}(\text{acac})_3$**

The solution of nanoparticles was digested with aqua regia overnight. The solutions were diluted with 1% nitric acid solution.

The conversion rate of  $\text{Fe}(\text{acac})_3$  was calculated by % Fe obtained in nanoparticles over the total % Fe in the reaction mixture.

$$\% \text{ Fe conversion} = \frac{[\text{Fe}] \text{ after purification}}{[\text{Fe}] \text{ before purification}} \times 100\%$$

#### **g. Determination of crystallite sizes of iron oxide nanoparticles**

The X-ray diffractograms were collected under Rigaku MiniFlex 600 X-ray Diffractometer (40 kV, 15mA) using Cu  $K\beta$  radiation ( $\lambda = 0.154$  nm). The scan degree was from  $10^\circ$  to  $80^\circ$ , step degree of 0.01 at the rate of  $1^\circ/\text{min}$ . Based on the strongest peak of (311), the crystal sizes of iron oxide nanoparticles were calculated according to Debye-Scherrer equation:  $D_{hkl} = k \lambda / \beta \cos\theta$ . Here  $D_{hkl}$  is crystallite size parallel to the ( $hkl$ ) plane,  $k$  is a constant of typical 0.89,  $\lambda$  is wavelength of X-ray source,  $\beta$  is full width at half maximum (FLHM) of diffraction peak, and  $\theta$  is angel of diffraction peak.

#### **h. Measurement of DEG density on the surface of iron oxide nanoparticles**

The sample was freeze-dried prior to analysis. An adequate amount of sample was placed in a platinum pan and heated from  $30^\circ\text{C}$  to  $800^\circ\text{C}$  at  $10^\circ\text{C}/\text{min}$  and 60 ml/min nitrogen gas flow. Data was analyzed using TA Universal Analysis (Version 4.5A, TA Instruments-Waters LLC).

The density of DEG on the surface of iron oxide nanoparticle was calculated according to the formula:

$$D = \frac{N(\text{DEG})}{S(\text{NP})} \quad (1)$$

$S(\text{NP})$  is surface area of each nanoparticle:

$$S(\text{NP}) = 4\pi r^2 \quad (2)$$

$r$  is radius of nanoparticle

$N$  (*DEG*) is the number of DEG molecules on each nanoparticle, which can be obtained by:

$$N(DEG) = \frac{m(DEG)}{Mw(DEG)} \times NA \quad (3)$$

$NA$  is avogadro's number,  $Mw$  is molecular weight of DEG which is 106.12.

$m$  (*DEG*) is mass of DEG on each nanoparticle:

$$m(DEG) = \frac{m(\text{weight loss from TGA})}{[1 - m(\text{weight loss from TGA})]} \times m(NP) \quad (4)$$

The mass of each nanoparticle is calculated from:

$$m(NP) = \frac{4}{3}\pi r^3 \times \rho \quad (5)$$

$\rho$  is density of bulk iron oxide which is 5.15 g/cm<sup>3</sup>

$r$  is radius of nanoparticle

#### **i. Stability study in water and PBS with different pH 5.4, 7.4, 9.0**

Purified samples were dispersed in 10 mM phosphate buffer solution (PBS) (from Sigma-Aldrich) with pH 5.4, 7.4 and 9. The change in hydrodynamic size of nanoparticles over time were studied using DLS. The photos of aqueous solution were taken over time.

#### **j. $T_1$ and $T_2$ measurement**

$T_1$  and  $T_2$  relaxation time of a series nanoparticles dispersion with different iron concentrations were measured with Siemens MAGNETOM Aera 1.5T MRI (Siemens Healthcare, Erlangen, Germany) clinical scanner. An  $T_1$  and  $T_2$  measurement protocol in the MRI system was used.[1]  $T_1$  weighted image was acquired by a 3D  $T_1$ -weighted gradient-echo echo pulse sequence at multiple flip angles (TR = 4.87 ms, first TE = 2.29 ms, slice thickness = 3.5 mm, flip angle 1 to 19 degree).  $T_2$ -weighted image was acquired by a 2D multi-echo  $T_2$ -weighted spin echo pulse sequence (TR = 2000 ms, 22 TEs from 10.6 ms to 233.2 ms, slice thickness = 5 mm). Both imaging field-of-view (FOV) was 256 x 128 mm and the matrix size was 256 x 128. The specific relaxivities

of  $r_1$  and  $r_2$  for nanoparticles were computed by taking the linear slope of  $1/T_2$  (or  $1/T_1$ ) versus Fe concentration.

#### **k. Magnetic properties**

The magnetic properties were performed by the superconducting quantum interference device (SQUID, Quantum Design, MPMS XL). Field cooled (FC) and Zero field cooled (ZFC) magnetization measurements under an applied field of 50 Oe in the temperature range of 5-300 K were performed as warming up. The field dependent magnetization measurements were conducted from -2.5 T to 2.5 T at 5 K and 300K, respectively.

#### **l. X-ray photoelectron spectroscopy (XPS)**

The XPS measurements were carried out using a ScientaOmicron ESCA 2SR X-ray Photoelectron Spectroscopy System equipped with a flood source neutralizer. Samples were loaded into the loadlock and pumped until the vacuum was below  $5 \times 10^{-7}$  mBar before they were transferred into the sample analysis chamber. All analysis were carried out with a Mono Al  $K\alpha$  x-ray source (1486.6 eV) at the power of 450W, and the pressure in the analysis chamber was maintained below  $3 \times 10^{-9}$  mbar. Both a survey scan and high resolution core level region scan of each element for all samples were recorded and calibrated with C-C bond of C1s peak at 284.8. The core level spectra were also deconvoluted to obtain chemical state information.

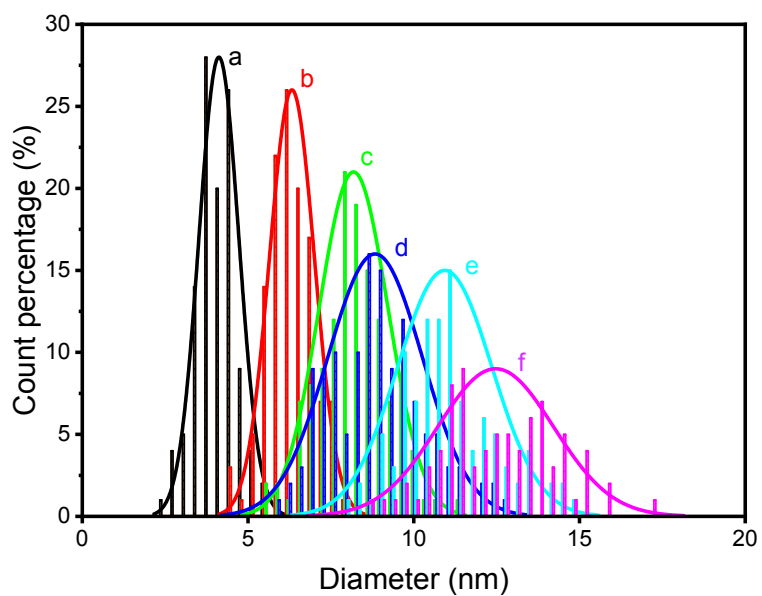


**Figure S1:** Histograms from the size analysis of iron oxide nanoparticles by TEM. The average sizes are (a)  $4.0 \pm 0.4$  nm, (b)  $6.2 \pm 0.5$  nm, (c)  $8.5 \pm 0.9$  nm, (d)  $9.3 \pm 1.1$  nm, (e)  $11.3 \pm 1.1$  nm, and (f)  $13.0 \pm 1.3$  nm.

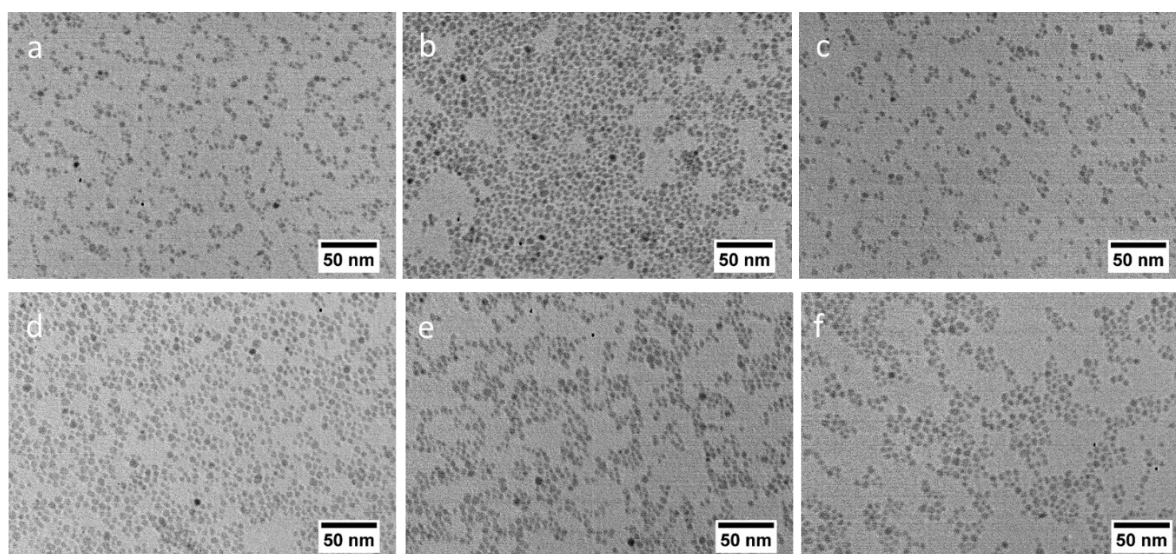


**Figure S2.** TEM images of iron oxide nanoparticles obtained at prolonged reaction time of (a) 0.5 h, (b) 1 h, (c) 2 h, (d) 3 h, (e) 4 h, and (f) 6 h. No reactant is added during the reaction. All scale bars are 50 nm.

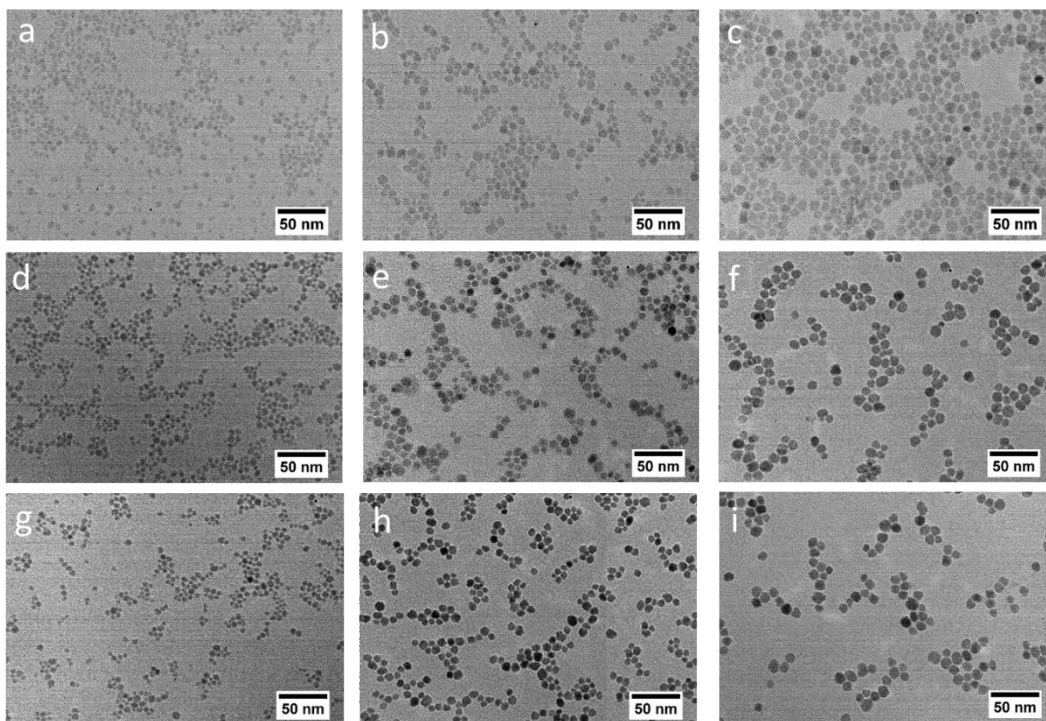


**Figure S3.** TEM images of iron oxide nanoparticles from three reactions to demonstrate reproducibility: the first reaction (a, b, c), the second reaction (d, e, f), and the third reaction (g, h, i); All scale bars are 50 nm.



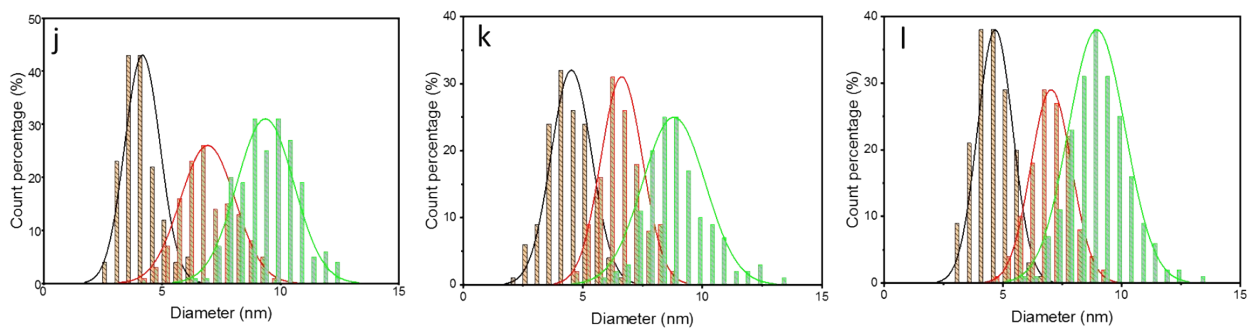


**Figure S4.** Histograms made from size analysis of iron oxide nanoparticles by TEM. The first reaction (j), the second reaction (k), the third reaction (l).

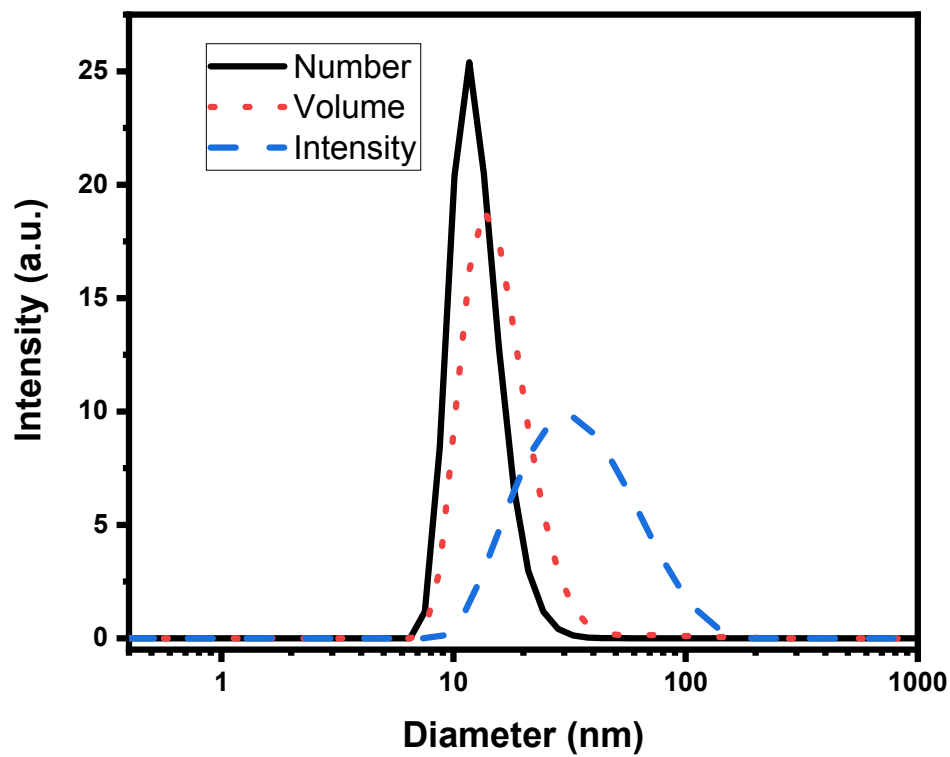


**Figure S5.** The narrow hydrodynamic size distribution of iron oxide nanoparticles by dynamic lighting scattering.

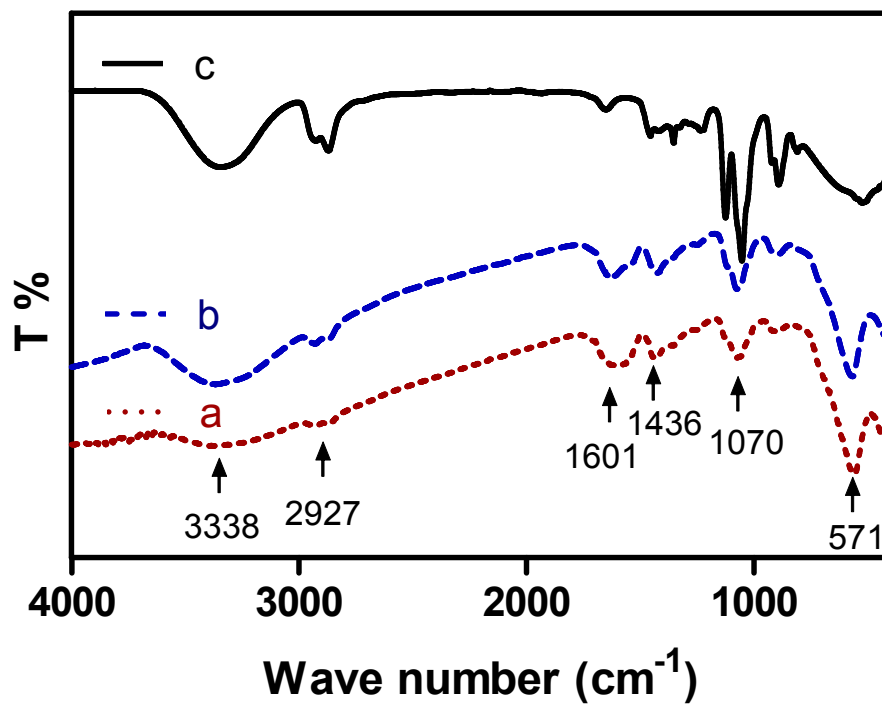


**Figure S6.** FT-IR spectra of iron oxide nanoparticles with the size of (a) 9 nm, (b) 4 nm, and (c) pure DEG.

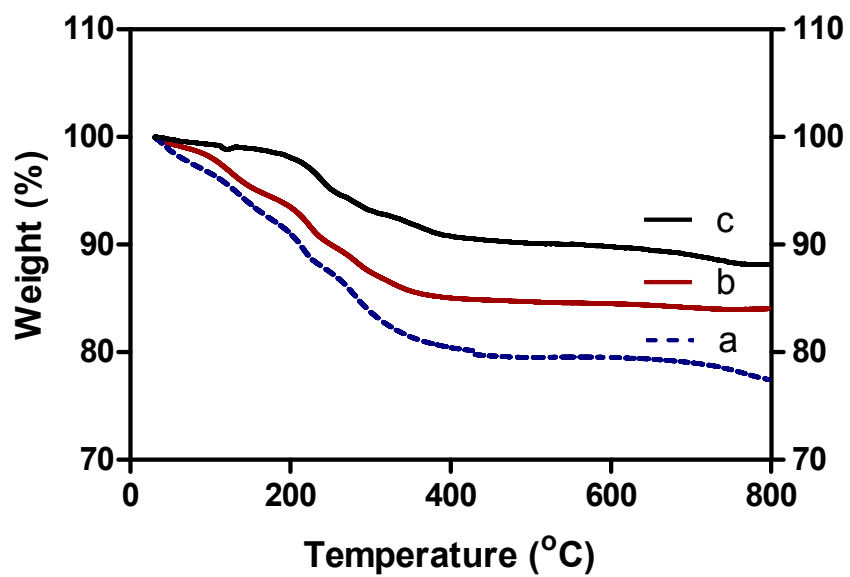


**Figure S7.** Thermal gravimetric analysis of iron oxide nanoparticles with size of (a) 4 nm, (b) 9 nm, and (c) 13 nm, showing weight percent (%) as a function of temperature (°C).

**Table S1:** Sizes of iron oxide nanoparticles synthesized by continuous growth from three reactions

<i>Reaction</i>	<i>The first growth Size (nm)</i>	<i>The second growth Size (nm)</i>	<i>The Third growth Size (nm)</i>
1	$4.2 \pm 0.7$	$6.9 \pm 1.2$	$9.5 \pm 1.4$
2	$4.5 \pm 0.8$	$6.6 \pm 0.9$	$8.8 \pm 1.3$
3	$4.6 \pm 0.7$	$7.0 \pm 0.9$	$9.0 \pm 1.2$

**Table S2.** Weight loss and DEG density for iron oxide nanoparticles with different sizes from TGA

Sample size	Weight Change (%)	DEG on surface (per nm <sup>2</sup> )
4 nm	12.7	3.0
9 nm	9.6	4.9
13 nm	8.4	5.8
Average		4.6

**Table S3.** Relaxivity properties of iron oxide nanoparticles of different sizes.

Size (nm)	$r_2$ (mM <sup>-1</sup> .s <sup>-1</sup> )	$r_1$ (mM <sup>-1</sup> s <sup>-1</sup> )	$r_2/r_1$
4	154.6	23.5	6.6
6	263.9	31.6	8.4
9	425.5	32.1	13.3

## **Reference**

[1] Keenan KE, Ainslie M, Barker AJ, Boss MA, Cecil KM, Charles C, Chenevert TL, Clarke L, Evelhoch JL, Finn P, Gembris D, Gunter JL, Hill DLG, Jack CR Jr, Jackson EF, Liu G, Russek SE, Sharma SD, Steckner M, Stupic KF, Trzasko JD, Yuan C, Zheng J. Quantitative magnetic resonance imaging phantoms: A review and the need for a system phantom. *Magn Reson Med.* 2018 79 (1):48-61.